

PWレーザー駆動高速点火プラズマにおけるMeV高速電子によるエネルギー  
輸送

**Energy transport by MeV hot electrons in fast ignition plasma driven with  
LFEX PW laser**

Z. Zhang<sup>1</sup>, 西村博明<sup>1</sup>, 藤岡慎介<sup>1</sup>, 有川安信<sup>1</sup>, 中井光男<sup>1</sup>, 尾崎哲<sup>2</sup>, 長友英夫<sup>1</sup>, H. Chen<sup>3</sup>, J. Park<sup>3</sup>, G.J. Williams<sup>3</sup>, 城崎知至<sup>4</sup>, 砂原淳<sup>5</sup>, 白神宏之<sup>1</sup>, 小島完興<sup>1</sup>, 宮永憲明<sup>1</sup>, 河仲準二<sup>1</sup>, 中田芳樹<sup>1</sup>, 實野孝久<sup>1</sup>, 疇地宏<sup>1</sup>  
Z. Zhang<sup>1</sup>, H. Nishimura<sup>1</sup>, S. Fujioka<sup>1</sup>, Y. Arikawa<sup>1</sup>, M. Nakai<sup>1</sup>, et. al.

阪大レーザー研<sup>1</sup>, 核融合研<sup>2</sup>, LLNL<sup>3</sup>, 広大<sup>4</sup>, レーザー総研<sup>5</sup>  
Osaka Univ. ILE<sup>1</sup>, NIFS<sup>2</sup>, LLNL<sup>3</sup>, Hiroshima Univ.<sup>4</sup>, ILT<sup>5</sup>

Fast ignition is recognized as a promising pathway to efficient thermonuclear fusion in laser-driven inertial confinement fusion. A cone-guided CD-shell has been used as a base-line target for the fast ignition realization [1, 2]. It has long been expected to provide more quantitative information about the hot electron generation and transport in the cone than those derived only with x-ray imaging and neutron detection. In this research, we propose an absolute  $K\alpha$  line spectroscopy dedicated for quantitative measurement of hot electron generation and transportation in high-Z targets. This diagnostic provides local information about the hot electrons propagating through specific materials composing the cone-guided target.

In this study, Au and Ta were chosen as tracers since they are representative highest-Z materials which are available for the guiding cone, thus better matching with MeV-hot electrons than lower-Z tracers such as Cu.

A Laue spectrometer was developed to cover the high energy  $K\alpha$  lines from Mo ( $K\alpha_1$ : 17.48 keV,  $K\alpha_2$ : 17.37 keV) to Au ( $K\alpha_1$ : 68.80 keV,  $K\alpha_2$ : 66.99 keV)[3]. The spectrometer consists of a cylindrically curved quartz (10-11) plate and a detector. The quartz plate is bent such that the diffracted x-rays are focused at an intermediate slit. X-ray components propagating in a straightforward manner are shielded from the detector directly with a lead pinhole plate located in front of the crystal and a pair of lead shields located at the intermediate x-ray focus. By varying the distances from the crystal to the source and detector, this spectrometer can cover the energy range of either 10-60 keV or 22-100 keV.

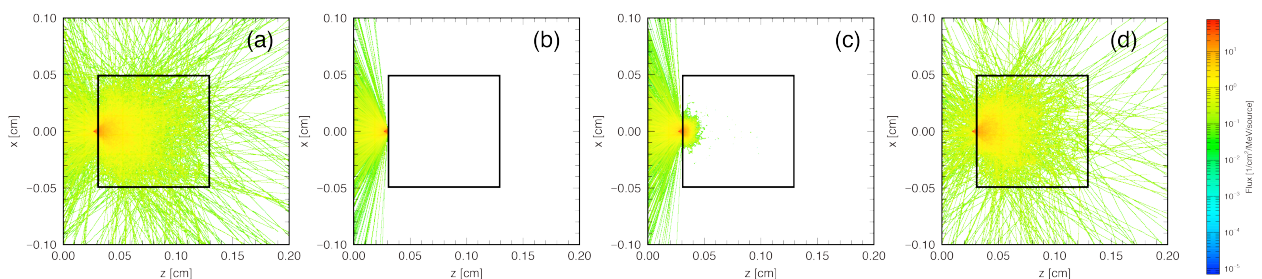


Fig. 1. Electron trajectory in the Ta cube: (a) all electrons, (b) electron with energy less than 0.1 MeV, (c) electron with energy from 0.1 to 1 MeV, (d) electron with energy more than 1 MeV.

The hot electron trajectory inside the solid target is tracked with Monte-Carlo simulation. A 3-dimensional code PHITS was applied. The code applies a continuous slowing down approximation (CSDA), which means that the electrons change their direction of motion due to elastic scattering, and lose their energy between two scattering points continuously. An example is shown in Fig. 1. The black square in the center indicates a 1 mm Ta cube, which is surrounded by low density air with a pressure of  $10^{-5}$  Torr. The hot electron beam was irradiated on the Ta cube from the left side. An initial divergence of  $45^\circ$  and a Gaussian spatial profile were assumed. The energy spectrum was set based on the electron spectrometer (ESM)

measurement in experiments. From Fig. 1, it is clearly seen that most of the electrons with energy less than 0.1 MeV were reflected at the front surface. The penetration depth increased along with electron energy; and only part of the electrons with energy higher than 1 MeV can propagate through the Ta cube and escape from the back surface.

The laser transfer efficiency,  $\eta_{TE}$ , is defined as the fraction of energy deposited into hot electrons. The number of  $K\alpha$  photons  $N_{K\alpha}$  generated from hot electrons with number  $N_h$  and temperature  $T_h$  can be estimated by the following model:

$$N_{K\alpha} = N_h \frac{n_A \omega_{K\alpha}}{4\pi T_h} \int_0^\infty dE \sigma_{K\alpha}(E) \times \int_0^d dx f_h(E_0, x) \exp\left(-\frac{x}{\lambda_{mfp} \cos(\theta)}\right) \quad (1)$$

where  $\sigma_{K\alpha}$ ,  $\omega_{K\alpha}$ , and  $n_A$  are, respectively, the cross section for K-shell ionization, the  $K\alpha$  fluorescence yield, and the atomic number density. The term  $\exp(-x/\lambda_{mfp} \cos(\theta))$  describes the reabsorption of  $K\alpha$  photons during the propagation through the target material, where  $\theta$  is the angle between the spectrometer and target normal.  $f_h(E_0, x)$  describes the energy spectrum for the hot electron propagating inside the Ta cube with a depth  $x$ , where the information was achieved with PHITS simulations. Considering the absolute  $K\alpha$  photon number  $N_{K\alpha}$  measured by the Laue spectrometer, the transfer efficiency  $\eta_{TE}$  can be estimated by comparing the experimental measurement and simulation results. The transfer efficiency from LFEX laser to target has been estimated in the cases of planar and cone-guided geometry. In the case of planar target, an Au plate was placed at the target chamber center and the LFEX laser with maximum energy of 1.8 kJ was focused on the front surface with an incident angle of  $10^\circ$ . The  $K\alpha$  from Au was recorded by the Laue spectrometer and an ESM was located from the back surface for the hot electron temperature. The  $\eta_{TE}$  as a function of laser intensity is shown in Fig. 2. As a general trend, the  $\eta_{TE}$  is increased by increasing the laser intensity.

The cone-guided configuration is shown in Fig. 3(a). A cone is attached with a hemi-CH shell, which was irradiated by three beams of Gekko-XII laser [1]. A dense plasma surrounding the tip of the cone was produced to mimic the condition of the fast ignition Au cone+CD shell target. The Ta cube was attached as the  $K\alpha$  tracer after the hemi-CH shell. Four types of cone were used, as shown in Fig. 3(b)-(e): (b) is the standard Au cone with  $7 \mu\text{m}$  thickness; (c) is the open-cone without tip; (d) is the W-cone with double Au layers; and (e) is the diamond like carbon (DLC) cone. The estimated  $\eta_{TE}$  was shown in Fig. 3. Compared with the planar geometry, the LFEX laser transfer efficiency is significantly enhanced with a guiding cone.

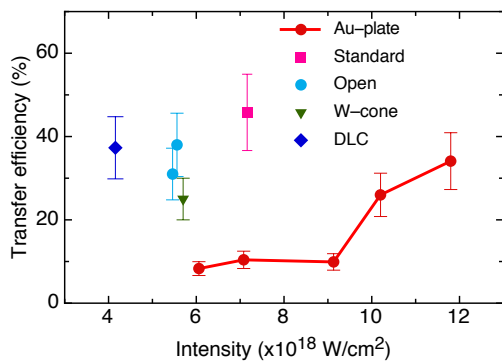


Fig. 2. The  $\eta_{TE}$  as a function of laser intensity for the planar and cone-guided targets.

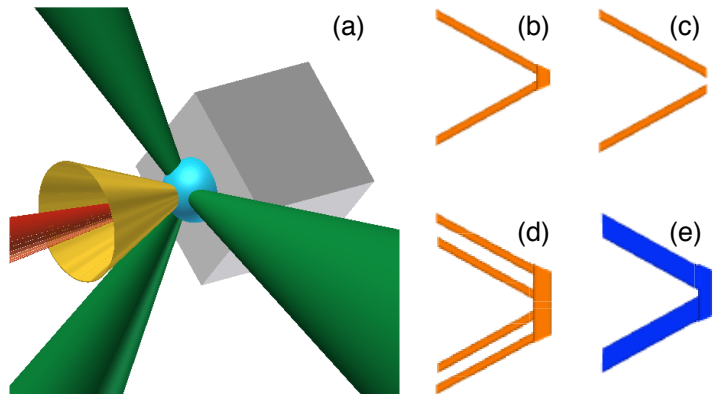


Fig. 3. (a). The configuration of a cone+CH hemi shell+Ta cube target; (b). Standard Au cone; (c). Open Au cone; (d). W-cone; (e). DLC cone.

- [1] H. Shiraga et. al., 2012 High Energy Density Phys. **8** 227  
[2] R. Kodama et. al., 2001 Nature **412** 798  
[3] Z. Zhang et. al., 2012 Rev. Sci. Instrum. **83** 053502